HHS Public Access

Author manuscript

J Bone Miner Res. Author manuscript; available in PMC 2018 June 01.

Published in final edited form as:

J Bone Miner Res. 2017 June ; 32(6): 1332–1342. doi:10.1002/jbmr.3112.

N-cadherin Regulation of Bone Growth and Homeostasis is Osteolineage Stage-Specific

Francesca Fontana[1], **Cynthia L. Hickman-Brecks**[1], **Valerie S. Salazar**[1,2], **Leila Revollo**[1,2], **Grazia Abou-Ezzi**[1,3], **Susan K. Grimston**[1], **Sung Yeop Jeong**[1], **Marcus Watkins**[1], **Manuela Fortunato**[1], **Yael Alippe**[1], **Daniel C. Link**[1,3], **Gabriel Mbalaviele**[1], and **Roberto Civitelli**[1]

[1]Department of Internal Medicine, Division of Bone and Mineral Diseases. Musculoskeletal Research Center, Washington University School of Medicine, St. Louis, MO USA

[2]Department of Development Biology, Harvard School of Dental Medicine, Boston, MA, USA

[3]Division of Oncology, Stem Cell Biology, Washington University School of Medicine, St. Louis, MO USA

Abstract

N-cadherin inhibits osteogenic cell differentiation and canonical Wnt/β-catenin signaling in vitro. However, in vivo both conditional *Cdh2* ablation and overexpression in osteoblasts lead to low bone mass. We tested the hypothesis that N-cadherin has different effects on osteolineage cells depending upon their differentiation stage. Embryonic conditional osteolineage *Cdh2* deletion in mice results in defective growth, low bone mass and reduced osteoprogenitor number. These abnormalities are prevented by delaying *Cdh2* ablation until 1 month of age, thus targeting only committed and mature osteoblasts, suggesting they are the consequence of N-cadherin deficiency in osteoprogenitors. Indeed, diaphyseal trabecularization actually increases when *Cdh2* is ablated postnatally. The sclerostin-insensitive $Lrp5^{A214V}$ mutant, associated with high bone mass, does not rescue the growth defect, but it overrides the low bone mass of embryonically *Cdh2* deleted mice, suggesting N-cadherin interacts with Wnt signaling to control bone mass. Finally, bone accrual and β-catenin accumulation after administration of an anti-Dkk1 antibody are enhanced in N-cadherin deficient mice. Thus, while lack of N-cadherin in embryonic and perinatal age is detrimental to bone growth and bone accrual, in adult mice loss of N-cadherin in osteolineage cells

Address all correspondence and reprint requests to: Roberto Civitelli, MD, Division of Bone and Mineral Diseases, Washington University in St. Louis, 660 South Euclid – Campus Box 8301, St. Louis, MO 63110, USA, civitellir@wustl.edu.

Contributions: F.F. designed and performed the work on constitutive and delayed *Cdh2* ablation and on MSPC, analyzed the entire dataset, and co-wrote the manuscript; C.H-B. performed the work with the $Lrp5^{A214V}$ mutant; L.R. designed and performed the experiments with *cKO-Prx1* mice; V.S. designed and performed experiments on the αDkk1 antibody; S.G and M.W. performed and analyzed μCT scans; S-Y.J. assisted with static histomorphometric and dynamic histomorphometric analysis and with genotyping; M.F. performed X-ray analysis of long bones; Y.A. assisted with gene expression analysis and genotyping; G.A.E. and D.L. assisted with the flow cytometry work and analysis; G.M. and R.C. conceived and supervised the entire experimentation. R.C. reviewed the entire data set and co-wrote the manuscript. D.L. and G.M. contributed to data analysis and interpretation and to manuscript editing. F.F. and R.C. take full responsibility for data integrity and analysis. This work was performed in partial fulfillment for the post-doctoral work of Francesca Fontana.

Conflict of Interest

Roberto Civitelli receives research support from Amgen, and holds stock of Amgen, Eli-Lilly and Merck & Co. Gabriel Mbalaviele is co-founder of Confluence Life Sciences. All other authors have no conflicts of interest.

favors bone formation. Hence, N-cadherin inhibition may widen the therapeutic window of osteoanabolic agents.

Introduction

Osteoporosis and consequent fragility fractures affect millions of people and represent an increasing burden for the health care system [1–3]. Pharmacologic agents that inhibit bone resorption significantly reduce bone loss and facture risk [4], but they cannot restore normal bone mass [1]. The Wnt signaling system, a key regulator of morphogenesis and tissue renewal [5], is the target of new osteo-anabolic agents [6,7]. The relevance of Wnt signaling to bone mass homeostasis is underscored by the high bone mass in sclerosteosis or Van Buchem disease, both caused by loss-of-function mutations of *SOST*, the gene encoding the Wnt inhibitor sclerostin [8]. Likewise, mutations that render the Wnt co-receptor *LRP5* insensitive to sclerostin and/or Dkk1, another Wnt inhibitor, cause high bone mass [6]. By constrast, *LRP5* loss-of function mutations result in osteoporosis pseudoglioma syndrome [9]. Accordingly, antibodies neutralizing sclerostin or Dkk1 have been successfully used to increase bone mass in experimental models [6,10]; and human antibodies against sclerostin are currently in phase III trials [11]. Nonetheless, there are still some unresolved issues about the mechanisms by which Wnt signaling activation alters bone remodeling, and how such modulatory actions can be used to achieve and optimize bone anabolism.

Cadherins are single chain integral membrane glycoproteins that mediate calcium-dependent cell-cell adhesion at adherens junctions [12,13]. The cytoplasmic tail is highly conserved among cadherins and binds β-catenin and plakoglobin, which link cadherin molecules to the actin cytoskeleton via α-catenin. Such interaction modulates the strength of the adhesion complex [14]. A growing body of evidence shows that in addition to their adhesive function cadherins interfere with Wnt signaling [13,15–17]. For example, N-cadherin binds to Lrp5/6 via axin, thus subtracting these co-receptors from Wnt signaling and favoring β-catenin degradation [16]. Accordingly, mice overexpressing N-cadherin in osteoblasts have low bone mass [16]. Indeed, our group reported that genetic ablation of the N-cadherin gene (*Cdh2*) in osteolineage cells enhances in vivo the bone anabolic response to intermittent parathyroid hormone (PTH) administration, an effect related to accentuated PKA-dependent β-catenin activation by PTH [18]. These results imply that N-cadherin restrains Wnt signaling in bone cells. However, our and others's work has also shown that either dominant negative disruption of cadherin function or *Cdh2* ablation in mice leads to low peak bone mass and osteopenia [19–21]. Intriguingly, the number of bone marrow stromal cells that have osteogenic capacity is decreased in *Cdh2* haploinsufficient or conditionally *Cdh2* ablated mice [20], pointing to a positive role of N-cadherin in the early phases of osteogenic development.

In this work, we tested the hypothesis that N-cadherin has a dual action in the osteolineage; it maintains the pool of osteoprogenitor and stem cells but it restrains differentiation and/or function of committed or mature osteoblasts via negative interference with Wnt signaling. We show that while embryonic *Cdh2* deletion in mice results in defective growth, low bone

mass and reduced osteoprogenitor number, such abnormalities are prevented by delaying *Cdh2* ablation until 1 month of age, when only committed and mature osteoblasts are targeted, suggesting they are the consequence of N-cadherin deficiency in the developing skeleton. On the other hand, a gain-of-function *Lrp5* mutant overrides the low bone mass of osteolineage-specific *Cdh2* deficient mice, but does not rescue the early growth defect. Finally, we find that N-cadherin deficient mice are hyper-responsive to anabolic signals induced by administration of an anti-Dkk1 antibody. These results explain the seeming paradox that both *Cdh2* deletion and overexpression result in low bone mass, and provide in vivo evidence in support of N-cadherin targeting to expand the anabolic window of Wnt signaling activators.

Materials and Methods

Animals

All the mouse models used here have been previously described. The tetracycline-responsive B6.Cg-Tg(Sp7-tTA,tetO-EGFP/cre)1Amc/J (Jackson laboratories) mice (*Osx-Cre*) were used to induce constitutive or delayed gene recombination. *Osx-Cre* mice were mated with $Cdh2^{flox/flox}$ ($Cdh2^{F/F}$) mice [22] to generate $Cdh2^{F/F}$::*Osx-Cre* mice (*cKO-Osx*), as previously described [18,21]. The reporter mice B6.Cg-Gt(ROSA)26Sortm9(CAG-tdTomato)Hze/J (Ai9), was purchased from Jackson Laboratories. Transgenic mice expressing *Cre* under the control of the 2.3-kb proximal fragment of the α*1(I)-collagen* promoter (*Col1A1*) [23] were crossed with $Cdh2^{F/F}$ mice to generate *2.3Col1A1-Cre*::$Cdh2^{F/F}$ (*cKO-Col1A1*) [20]. Similarly, $Cdh2^{F/F}$ were crossed to *Prx1-Cre*, kindly provided by Dr. David M. Ornitz (Washington University), to generate *Prx1-Cre*::$Cdh2^{F/F}$ (*cKO-Prx1*) [24]. Mice with a germline $Lrp5^{A214V}$ mutant allele (a generous gift from Dr. Matthew L. Warman, Harvard University), which renders the co-receptor resistant to Dkk1and sclerostin inhibition and is associated with high bone mass [25], were bred with *Osx-Cre* and $Cdh2^{F/F}$ mice to generate mice in which *Cdh2* was conditionally deleted while one allele of $Lrp5^{A214V}$ was globally expressed (*cKO-Osx*;$Lrp5^{A214V/+}$). Unless otherwise indicated, $Cdh2^{F/F}$ littermates were used as controls. Genotyping was performed by PCR on genomic DNA extracted from mouse tails using the HotSHOT method. Primers to detect $Cdh2^{F}$ [20], *2.3Col1A1-Cre* [26], *Osx-Cre* [18], and $Lrp5^{A214V}$ [25] alleles have been described previously. Mice were fed an ad libitum regular chow (PicoLab Rodent Diet 20, 5053; TestDiet/LabDiet, St. Louis, MO) and housed in cages containing 2–5 animals each, in a room maintained at constant 25°C on a 12-hour light/dark cycle. In some experiments, a chow containing doxycycline (Doxy; 200 ppm) was used (Modified LabDiet 5058, 5BFB). All procedures were approved by the Animal Studies Committee of Washington University.

Reagents

Rat monoclonal anti-mouse Dkk1 neutralizing antibody (αDkk1; clone 11H10) was a kind gift of Dr. William Richards, Amgen, Inc. (Thousand Oaks, CA). αDkk1 was prepared in sterile saline and administered at 20 mg/kg/day via i.p. injections, 3 times a week for 4 weeks. Antibodies for immunoblotting were purchased from commercial sources, specifically: β-actin (Sigma-Aldrich, St. Louis, MO; cat# A5316), and N-cadherin (BD Biosciences, Franklin Lakes, NJ, USA; cat# 610920).

Calvaria organ cultures

Sagittal halves of neonatal mouse calvaria were cultured for nine days in basic media (no FBS) plus osteogenic cocktail in the presence or the absence of 100 or 200 ng/ml αDkk1. New bone tissue was labeled on day 10 by labeling overnight with 20 μM xylenol orange in culture media. Images of Ai9/Osx-cre parietal bones were acquired on day 0 of *ex-vivo* organ culture in basic media as phase contrast and red fluorescence, and then merged in ImageJ software (National Institutes of Health, USA).

Bone imaging and microstructure

For ex-vivo imaging, dissected bones were fixed in 10% buffered formalin and kept in 70% ethanol. Digital contact radiographs were taken using a Faxitron UltraFocus100 scanner (Faxitron Bioptics, LLC Tucson, AZ, USA). Tibial length was measured in blind using the instrument's acquisition software (Vision Version 2.3.1, Faxitron). For in vivo analysis of bone microstructure and mineralization, animals were subjected to in vivo scanning using μ-CT (VIVA CT40, Scanco Medical, AG, Switzerland) and previously described parameters [27]. Microstructural analysis of cancellous and cortical bone was also as described [27,28]. For ex-vivo μCT analysis, tiabiae or femurs were frozen until use, then placed in 2% agarose gel and scanned using a μCT system (μCT- 40, Scanco Medical) as previously described [20,21]. Diaphyseal trabecularization was measured in scans of whole tibiae as the distance between the proximal growth plate and the most distal trabeculae, normalized to diaphyseal length (distance between growth plates).

Flow cytometry

Whole bones (tibia, femur and pelvis) of 3-week-old pups were smashed in PBS, digested with 1.67 mg/ml of type II collagenase (Worthington Biochemical, Lakewood, NJ, USA) in phosphate-buffered saline (PBS) for 12 min at 37°C and filtered. Samples were tested for viability, and stained for CD45 (BD-Bioscience, clone: 30-F11), Ter119 (BD, clone: TER-119), CD31 (BD, clone: 390), PDGFRβ (eBioscience, clone: APB5), and Sca-1 (BD, clone: D7), using previously described protocols [29]. About 10^6 events per sample were acquired with a FACSscan cytometer, and analyzed with FlowJo 10.0.7 software (TreeStar/FlowJo LLC, Ashland, OR, USA). In the CD45− Ter119− CD31− gated cells, PDGFRβ+ Sca-1+ (PβS) cells were considered to be enriched in mesenchymal stem and precursor cells (MSPC). Although PDGFRα is more commonly used as a marker of MSPC [30], PDGFRβ expression largely overlaps with PDGFRα (Link et al. unpublished observations), and the anti-PDGFRβ we use has better sensitivity and specificity than anti-PDGFα antibodies.

Bone histology and histomorphometric analysis

Bone samples were prepared as previously described [28]. For dynamic histomorphometry, mice were injected with calcein (15 mg/kg i.p., Sigma-Aldrich) 7 and 3 days before euthanasia to label mineralizing fronts. Undecalcified long bones were embedded in methyl methacrylate and 4 μm thick longitudinal sections of the whole bone were cut and left unstained for assessment of calcein fluorescence. Quantitative histomorphometry was performed using a commercial software (OSTEO II, Bioquant, Nashville, TN, USA), and standard parameters of bone remodeling were determined according to the American Society

for Bone and Mineral Research guidelines [31]. Representative images of the femoral metaphysis were acquired at 40× magnification with an Axiovert S100 fluorescent microscope (Zeiss, Jena, Germany).

Cell culture

Bone marrow stromal cells were obtained by flushing bone marrow from long bones as previously described [20,32], filtering the re-suspended marrow with a 70μm cell strainer, and diluting in culture media containing ascorbic acid-free α-MEM (Invitrogen) with 40 mM L-glutamine, 100 U/ml penicillin-G, 2.5 μg/mL amphotericin B, 100 mg/ml streptomycin, and 15% FBS (culture media). Cell cultures were incubated at 37°C in a humidified atmosphere with 5% CO_2, and culture media replaced every 3–5 days. To determine the number of colony forming units - fibroblasts (CFU-F), serial dilutions of bone marrow cells were cultured in culture media for 15–20 days, fixed in ethanol, and stained with Giemsa as previously described [33]. For osteogenic differentiation, cells were cultured for 21–28 days in an osteogenic cocktail (50 μg/ml ascorbic acid and 10 μM β-glycerophosphate) [33], and stained for alkaline phosphatase using the Leukocyte Alkaline Phosphatase kit (Sigma) or alizarin red (0.4% after fixation in ethanol 70%) as previously described [32,33]. Alkaline phosphatase or Giemsa positive colonies were counted at low magnification by a blinded observer for assessment of CFU-alkaline phosphatase (CFU-AP). Alizarin stained areas in each well were quantified in scanned images using ImageJ. For biochemical assays, 5×10^5 bone marrow stromal cells were cultured for 5 days in media with osteogenic cocktail, then mechanically harvested in ice-cold PBS [20,32].

Biochemical markers of bone turnover

Serum was obtained from mice that had been deprived of food and water for 6 hours before sacrifice. As a marker of bone formation, serum levels of N-terminal pro-peptide of human pro-collagen type I (P1NP) were determined with Rat/Mouse P1NP EIA (Immunodiagnostic Systems, The Boldons, UK; Cat. AC-33F1), as previously detailed [28]. Procedures and data analyses were performed per manufacturer's instructions.

Western blots

Following previously detailed methods [18,34], cell extracts were lysed in RIPA buffer (50 mM Tris-HCl pH 8.0, 150 mM NaCl, 1 mM EDTA, 1% NP-40, 0.5% sodium deoxychlate, 0.1% SDS) with protease/phosphatase inhibitors (Thermo Scientific, Waltham, MA, USA; cat# 78443), sonicated and centrifuged at 12,000g for 10 minutes. Total protein concentration was determined with the *DC™* (detergent compatible) protein assay kit (BioRad, Hercules, CA, USA; cat# #500-0113, #500-00114, and #500-00115). For western blot analysis, a total of 5 μg of total protein was loaded on 10% acrylamide gels and separated by SDS-PAGE electrophoresis, then transferred to Immobilon membranes (Milipore, Billerica, MA, USA; cat# IPVH00010). Antigen-antibody complexes were visualized by incubation of the blots in a dilution of horseradish peroxidase-conjugated antibodies and ECL detection system (Millipore).

Statistics

For in vivo animal experiments, power analysis revealed that an n=8 was sufficient to detect 20% difference in volumetric bone volume/total volume by μCT (the main outcome variable) at 80% power and p=0.05 significance level. Lower sample sizes are reported in some circumstances because of problems with sample processing, or animal attrition during the observation period. In vivo experiments on adult animals were performed on both genders and analyzed separately, as indicated. Data from pups (aged <1 month) of both genders were pooled. Group means were analyzed by either Student's t test or analysis of variance (ANOVA) followed by post hoc analysis for multiple group comparisons using either Dunnett or Bonferroni tests. For samples with unequal variances or with numerical values =0, the non-parametric Wilcoxon rank test was used. Analyses were performed using SigmaPlot Vs11.0 (Systat, San Jose, CA, USA) or Prism 5 (GraphPad Software, Inc., La Jolla, CA, USA). Data are expressed as mean ± standard deviation.

Results

Embryonic but not postnatal *Cdh2* ablation causes stunted growth and low bone mass

We have previously shown that mice with *Cdh2* ablation in the osteogenic lineage driven by either the 2.3kb*Col1A1* or *Osx* promoters have low bone mass and smaller bones [20,21]. Consistently, *Osx-cKO* pups are smaller than $Cdh2^{F/F}$ littermates (Fig. 1A). The small body frame is present at birth, and remains evident during the first month of life resulting in short nose-tail length (Fig. 1B), short tibiae (Fig. S1A, B) and femurs (Fig. 1C), and significantly reduced body weight (20–29%), relative to $Cdh2^{F/F}$ littermates (Fig. 1D). While aging these attenuates differences, *cKO-Osx* mice remain smaller than normal throughout their life (not shown). Although *Osx* is expressed in committed and differentiated osteoblasts, during embryonic and early post-natal life *Osx-Cre* also targets cells with definitive stem cell capacity [35]. We leveraged the tetracycline-responsive element in the *Osx-Cre* transgene to delay Cre activation and *Cdh2* ablation until after birth. To validate the system, we first crossed *Osx-Cre* to Ai9 reporter mice (Ai9:*Osx-Cre*). A large proportion of cells (osteocytes or osteoblasts) in 2-month old *cKO-Osx* mice calvaria display red (TdT+) fluorescence (Fig. S1C). By contrast, very few osteocytes are TdT+ in calvaria from pups kept on Doxy. However, in 2-month-old *Ai9:Osx-Cre* mice kept on Doxy until weaning (about P28), and then taken off Doxy to allow Cre activation, most calvaria cells are TdT+; very similar to mice that continuously expressed *Osx-Cre* (Fig. S1C). Likewise, flow cytometry of bone marrow cells reveals very few TdT+ cells in Doxy-treated Ai9:Osx-Cre mice, while a significantly higher number is evident 1 month after Doxy withdrawal (Fig. S1D). Therefore, Doxy suppression of *Osx-Cre* until weaning prevents gene recombination, which efficiently occurs after antibiotic withdrawal, as previously published [35]. In *cKO-Osx* mice this is associated with detection of the *Cdh2* recombined allele in the calvaria of 2-month-old mice treated with Doxy until 1 month of age (Fig. S1E). Doxy-treated 10-day-old *cKO-Osx* pups are the same length as $Cdh2^{F/F}$ littermates, as opposed to significantly smaller *cKO-Osx* mice from dams fed a regular chow (Fig. 1E). Tibial morphology (S1F) and body weight of Doxy-treated *cKO-Osx* pups (S1G) are also indistinguishable from $Cdh2^{F/F}$ littermates or non-Doxy treated $Cdh2^{F/F}$ mice. Importantly, despite effective *Cdh2* ablation after Doxy withdrawal (see above), tibial morphology and length are normal in 3-month-old

Doxy-treated *cKO-Osx* (Fig. 1F, G); body weight is also normal in adult Doxy-treated *cKO-Osx* mice, whereas non-Doxy treated *cKO-Osx* mice are smaller than $Cdh2^{F/F}$ mice (Fig. 1H). Thus, *Cdh2* ablation after 1 month of age does not cause the growth defect that is consistently observed upon *Cdh2* deletion in the embryonic and perinatal period.

We have previously reported that *cKO-Osx* mice have low bone mass [18,21]; however, 2-month-old *cKO-Osx* mice treated with Doxy until 1 month of age have normal trabecular bone structure (Fig. 2A), trabecular bone volume (BV/TV, Fig. 2B) and bone mineral density (BMD) by μCT (Fig. S2A), compared to $Cdh2^{F/F}$ littermates. In fact, the extent of trabeculation in the metaphysis and diaphysis of the tibia is significantly greater in Doxy-treated *cKO-Osx* than in Doxy-treated $Cdh2^{F/F}$ mice (Fig. 2C). Furthermore, while *cKO-Osx* mice have smaller and thinner cortices [20,21], cortical BMD and thickness are normal in Doxy-treated *cKO-Osx* mice (Fig. S2B, C), Of note, transient low body weight and delayed cortical bone development have been observed in very young *Osx-Cre* mice, but these abnormalities resolve by 12 weeks of age [36], whereas low body weight, growth defect and osteopenia persisted at least up to 4 months of age in *cKO-Osx* mice. Therefore, it is unlikely that the observed phenotype be substantially affected by the *Osx-Cre* transgene itself.

To corroborate the notion that osteopenia in *Cdh2* ablated mice is related to a defect in osteogenic precursors, we used *Prx1-Cre* to inactivate *Cdh2* (*cKO-Prx1*) in mesenchymal precursors. Validating the system, no N-cadherin specific immunofluorescence staining is present in sections of cortical and trabecular limb bone of *cKO-Prx1* mice (Fig. S2D). Furthermore, N-cadherin protein is absent in bone marrow stromal cells of *cKO-Prx1* kept in osteogenic medium, whereas in $Cdh2^{F/F}$ mice N-cadherin is present during the first week of culture, and is down-regulated after 3–4 weeks in culture [18] (Fig. S2E). Although *cKO-Prx1* mice have normal body weight (Fig. S2F), possibly because of a more restricted field of expression of *Prx1* relative to *Osx*[37], they have significantly decreased BV/TV (Fig. 2D) and bone mineral density (BMD) by μCT (Fig. S2G). Accordingly, trabecular number is decreased (Fig. 2E) in *cKO-Prx1* mice, whereas trabecular thickness is normal (Fig. S2H), and trabecular spacing is increased (Fig. S2I). Total cortical area at the tibial mid-shaft is slightly but not significantly lower in *cKO-Prx1* mice (Fig. 2F). Only males were used in these experiments.

Cdh2 ablation early in the osteolineage results in low MSPC number

We have previously reported a reduced number of CFU-O in both *Cdh2* haploinsufficient [38] and *CKO-Col1A1* mice [20]. Corroborating this premise, the number of PβS cells, which have immunophenotypic features of mesenchymal stem cells [21,35], is lower in the bone marrow of 3-week-old *cKO-Osx* mice relative to $Cdh2^{F/F}$ mice (Fig. 3A, B). Accordingly, CFU-F, representing the number of mesenchymal precursors, and CFU-AP, representing chondro-osteogenic precursors, are significantly (about 80%) reduced in *cKO-Osx* relative to $Cdh2^{F/F}$ mice (Fig. 3C, D). Importantly, there is no significant difference in CFU-F between Doxy-treated *cKO-Osx* and $Cdh2^{F/F}$ mice 1 month after Doxy withdrawal (Fig. 3E, F), suggesting that loss of colony formation capacity is due to a cell autonomous defect in N-cadherin deficient mice. The mineralization capacity of bone marrow stromal

cells from Doxy-treated *cKO-Osx* mice is also non-inferior compared to Doxy-treated $Cdh2^{F/F}$ mice (Fig. 3F, G). Therefore, delaying *Cdh2* deletion until adult age prevents not only the low body weight and bone mass phenotype, but also the osteoprogenitor abnormality, suggesting that these actions of N-cadherin action occur on embryonic and/or perinatal MSPC, rather than adult osteoblasts.

The gain-of-function $Lrp5^{A214V}$ mutant fully rescues the low bone mass but not the growth defect of *cKO-Osx* mice

We and others have shown that N-cadherin inhibits the differentiation of committed osteogenic cells [20,39], and prevents the osteoanabolic effect of PTH via interference with Lrp6 signaling [18]. We used a genetic approach to directly test, in vivo, whether N-cadherin interferes with Lrp5/6 signaling by crossing *cKO-Osx* and $Lrp5^{A214V/+}$ mice. At 2 months of age, body weight is lower in both *cKO-Osx* and the compound *cKO-Osx;*$Lrp5^{A214V/+}$ mutants, relative to either $Cdh2^{F/F}$ or $Lrp5^{A214V/+}$ groups (Fig. 4A). Likewise, the length of tibial diaphysis is lower in *cKO-Osx* vs. $Cdh2^{F/F}$, and in *cKO-Osx;* $Lrp5^{A214V/+}$ vs. $Lrp5^{A214V/+}$ (Fig. 4B). However, 2-month-old *cKO-Osx* mice have lower BV/TV (Fig. 4C) and volumetric BMD relative to $Cdh2^{F/F}$ mice (Fig. 4D). As expected, BV/TV is significantly higher (almost 2-fold) in $Lrp5^{A214V/+}$ relative to $Cdh2^{F/F}$ mice; importantly, in double *cKO-Osx;* $Lrp5^{A214V/+}$ mutant mice BV/TV is not only higher than in $Cdh2^{F/F}$ mice, but it is almost 4-fold higher than in *cKO-Osx* mice (Fig. 4C). Volumetric BMD follows the same pattern (Fig. 4D). Lower bone mass in *cKO-Osx* mice is associated with lower trabecular number and higher trabecular spacing, with a trend towards lower trabecular thickness (Fig. S3A-C). On the other hand, the higher bone mass in $Lrp5^{A214V/+}$ and double mutant mice is associated with increased trabecular thickness, but no changes in trabecular number or spacing relative to $Cdh2^{F/F}$ mice (Fig. S3A-C). Cortical thickness is significantly increased in both $Lrp5^{A214V/+}$ and double mutants (Fig. 4E), with no changes in cross-sectional area or marrow area (Fig. S3D, E). Serum P1NP, a marker of bone formation, is higher in both $Lrp5^{A214V/+}$ groups, although the difference reaches statistical significance only in *cKO-Osx;* $Lrp5^{A214V/+}$ relative to $Cdh2^{F/F}$ and *cKO-Osx* mice (Fig. 4F). Dynamic histomorphometry shows significantly lower bone formation rate in *cKO-Osx* vs. $Cdh2^{F/F}$ mice (Fig. 4G); whereas mineralizing surfaces and mineral apposition rates are not different among groups (Fig. S3F, G). Notably, there is no double labelled surfaces in 75% of *cKO-Osx* mice, while *cKO-Osx;* $Lrp5^{A214V/+}$ bones exhibit distinct double calcein labeling (Fig. 4H). Thus, constitutive activation of Lrp5 signaling overrides the low bone mass phenotype of N-cadherin deficiency, but does not prevent the early growth defect.

Cdh2 ablation in osteoblasts enhances trabecular bone accrual in response to anti-Dkk1 antibody administration

Having shown that N-cadherin action on bone mass acquisition is, at least in part, dependent on Wnt signaling, we next asked whether *Cdh2* ablation in bone forming cells enhances the osteoanabolic response to acute, pharmacological activation of Wnt signaling, as it would be predicted by N-cadherin's inhibitory effect on Lrp5/6 [16,40]. To this end, we systemically administered a neutralizing αDkk1-antibody, which we have shown to increase bone mass in mice [10]. To verify that the antibody directly acts on bone cells in a dose-dependent manner, we isolated and cultured wild type mouse calvaria in the presence of different doses of

αDkk1 for 7 days, and observed abundant new bone deposition, visualized by xylenol orange stain, and increased calvaria thickness (Fig. S4A). In vivo, administration of 5 mg/kg αDkk1 for 4 weeks increases BV/TV in *cKO-Col1A1* relative to vehicle-treated *CKO-Col1A1* mice, which are osteopenic [20], but not in $Cdh2^{F/F}$ mice (Fig. 5A). On the other hand, comparable responses between the two genotypes are achieved with a higher dose (20 mg/kg) of the antibody (Fig. 5A). Accordingly, the higher dose of αDkk1 induces a significant increase in trabecular number (Fig. 5B), and a decrease in trabecular spacing only in *cKO-Col1A1* mice (Fig. 5C); while no significant changes are observed in trabecular thickness (Fig. 5D). The effects of high dose αDkk1 follow similar trends, but are non-significant in $Cdh2^{F/F}$ mice. No significant changes in cortical parameters, including total cortical and marrow area are noted after αDkk1 treatment in either genotype (Fig. S4B, C). Data are shown for male mice, but similar results were obtained in females.

Discussion

This work demonstrates that N-cadherin has a dual action in the osteolineage; it maintains the pool of osteoprogenitor cells but it restrains differentiation and/or function of committed and mature osteoblasts via negative interference with Wnt signaling. Our results provide an explanation to the paradox that both genetic ablation and overexpression of *Cdh2* result in low bone mass [18,20], and set the stage for a more accurate targeting of N-cadherin to achieve bone anabolic effects via Wnt signaling modulation.

Evidence has accumulated indicating that in committed osteogenic cells N-cadherin is an inhibitor of osteogenic differentiation and bone formation. In vitro, N-cadherin abundance decreases during osteoblast differentiation [18,20], which is instead enhanced in conditionally *Cdh2* ablated and haploinsufficient cells [20,38]; and inhibits expression of osteogenic target genes, thus hindering osteoblast proliferation and survival [15,16,41]. Accordingly, transgenic expression of *Cdh2* in differentiated osteoblasts interferes with bone formation resulting in low bone mass [16]. On the other hand, using different genetic models of conditional *Cdh2* ablation in osteogenic cells and dominant negative interference with N-cadherin function we have consistently observed reduced bone mass [19–21], and shorter, smaller long bones [20]. This study provides a mechanistic explanation to the apparent paradox; while bone mass is decreased and growth stunted when *Cdh2* is constitutively ablated by *Osx-Cre* – which targets osteoblasts and a subset of bone marrow stromal cells with MSPC features during embryogenesis and perinatal life [35] – such phenotype is prevented by delaying *Osx-Cre* activation until 4 weeks of life, when *Osx-Cre* only targets committed osteogenic cells. Therefore, the low bone mass and stunted growth is the consequence of loss of N-cadherin action on osteoprogenitors during embryogenesis or perinatal life. In support of this notion, we also show that *cKO-Osx* mice have fewer bone marrow PβS cells and reduced colony forming capacity in vitro, an abnormality that is also prevented by delaying *Cdh2* ablation postnatally. Indeed, we had observed reduced osteoprogenitor number in *Cdh2* haploinsufficient [38] and *cKO-Col1A1* mice [20]; and abnormalities of MSPC number and/or lineage allocation had also been reported upon dominant negative interference with osteoblast N-cadherin [19]. Thus, N-cadherin is involved in maintaining the pool of MSPC in the embryonic and perinatal period; loss of *Cdh2* leads to reduced MSPC and osteogenic (and possibly chondrogenic) cells, in turn resulting in stunted growth and low bone mass.

Therefore, the action of N-cadherin on MSPC, where it contributes to their maintenance, is distinct from its action on committed osteogenic cells, where it inhibits their function.

The concept that N-cadherin abundance must be kept at an appropriate level to maintain MSPC number and allow their differentiation had emerged from earlier in vitro data. During early stages of endochondral bone formation, high expression of N-cadherin favors embryonic mesenchymal micromass condensation [42,43], but N-cadherin must be down-regulated after condensation to allow chondrogenic differentiation to proceed [44]. In fact, a defect in chondrogenesis may explain, at least in part, the stunted longitudinal bone growth in *cKO-Osx*. The mechanisms by which N-cadherin controls MSPC number remains to be determined. N-cadherin inhibits Wnt/β-catenin signaling; accordingly, lack of N-cadherin enhances Wnt signaling responses, in vitro and in vivo [16,18]. Inhibition of Wnt signaling decreases mesenchymal stem cells survival and osteo- and chondrogenic differentiation [45]; thus, hyper-activation of Wnt signals in N-cadherin deficient MSPC may interfere with self-renewal and/or accelerate differentiation thus causing MSPC exhaustion. Alternatively, loss of N-cadherin adhesive function may contribute to MSPC loss in *Cdh2* deficient mice; N-cadherin-mediated cell-cell adhesion enhances expression of VCAM-1 and PDGFRβ, a marker of MSPC, and decreases cell motility and proliferation [46]. In any case, loss of MSPC in embryonic/perinatal life is likely the cause of low bone mass in conditionally *Cdh2* ablated mice, since both can be prevented by delaying *Cdh2* inactivation until 1 month of age.

The inhibitory function of N-cadherin on Wnt signaling, amply proven in vitro [15,16,18], would predict that N-cadherin deficiency in bone forming cells enhances the osteo-anabolic effect of Wnt activators in vivo. This prediction is fully borne out by our results showing that *cKO-Col1A1* mice exhibit increased sensitivity to pharmacologic Wnt activation, in that they accumulate bone mass after treatment with a dose of the αDkk1 antibody that is not effective in wild type mice. Furthermore, the Dkk1-resistant and sclerostin-insensitive $Lrp5^{A214V}$ mutant fully overrides the low bone mass phenotype of *cKO-Osx* mice, suggesting that Lrp5 signaling is dominant and that N-cadherin interacts with Wnt signaling in modulating bone mass. If N-cadherin acted independently of Wnt signaling, we would have expected bone mass in the *cKO-Osx;* $Lrp5^{A214V/+}$ double mutants be intermediate between that of $Lrp5^{A214V/+}$ and *cKO-Osx* mice. Reflecting enhanced osteogenic Wnt signaling response, circulating P1NP levels were higher in the double mutants relative to $Lrp5^{A214V/+}$ mice.

Our study also demonstrates for the first time in vivo that lack of N-cadherin in mature osteolineage cells leads to increased trebecular bone, thus corroborating the in vitro evidence that N-cadherin is a negative regulator of osteoblast function [15,38]. Consistent with this notion, *cKO-Col1A1* mice exhibit large bone gains in response to doses of systemically administered αDkk1 that are ineffective in non-deleted mice. The finding that postnatal *Cdh2* ablation does not cause osteopenia, but rather increases long bone trabeculation also implies that the two actions of N-cadherin, support of MSPC and inhibition of osteoblast function, are separable. This premise is further supported by the failure of the $Lrp5^{A214V}$ mutant to rescue the growth defect, while it fully rescues the low bone mass of *cKO-Osx* mice. Consistently, others have shown that transgenic overexpression of *Cdh2* in mature

osteoblasts causes osteopenia, but has no effect on early stages of skeletal growth [41]. Thus, through pharmacologic and genetic approaches, our results provide in vivo proof that N-cadherin restrains osteo-anabolic Wnt signals. Hence, inhibition of N-cadherin might be used to amplify the anabolic action of Wnt activators without negative effects on bone accrual and growth; low bone mass, decreased MSPC numbers and stunted growth are derived from *Cdh2* inactivation in the embryonic/perinatal period.

Anti-sclerostin antibodies have been developed as anabolic agents for osteoporosis; among those antibodies, romosozumab has completed phase III trials and demonstrated effectiveness in increasing bone mass [11,47]. However, while romosozumab rapidly uncouples bone formation and resorption in a positive fashion, bone turnover recouples within 6 months of therapy and resets below baseline after one year of treatment [11]. Increased circulating levels of sclerostin and Dkk1 have been reported in coincidence with reversal of bone formation rates following administration of other anti-sclerotin antibodies in humans [48] and ovariectomized rats [49], probably reflecting a homeostatic adaptation to Wnt activation caused by sclerostin neutralization. In this context, the possibility of modulating the sensitivity of osteogenic cells to Wnt activators by interfering with N-cadherin could be used to prolong anabolic responses to Wnt activators, similar to what we have shown for the anabolic effect of parathyroid hormone [18]. Indeed, preliminary data in mice suggest that pharmacologic interference with N-cadherin/Lrp5/6 interaction results in enhanced bone formation [50].

In summary, this study shows that N-cadherin is an important regulator of the osteogenic lineage; it maintains the pool of osteoprogenitor cells but it restrains the function of mature osteoblasts via negative interference with Wnt signaling. The low bone mass resulting from genetic ablation of *Cdh2* is likely related to a decreased number of osteogenic precursors, but it can be prevented by delaying *Cdh2* deletion until after weaning. On the other hand, mice lacking N-cadherin in osteogenic cells are hyper-responsive to Wnt-dependent osteo-anabolic signals. Our data provide a rationale for targeting N-cadherin to enhance the bone remodeling response to osteoanabolic agents, an action that could be useful in patients with low bone mass and increased fracture risk.

Supplementary Material

Refer to Web version on PubMed Central for supplementary material.

Acknowledgments

We thank the Musculoskeletal Histology, and Morphometry, and the Structure and Strength Cores of Washington University Musculoskeletal Research Center. This work was supported by grants from NIH/NIAMS R01-AR055913 (to RC), NIH/NIAMS P30-AR057235 (Core Center for Musculoskeletal Biology and Medicine), and Barnes-Jewish Hospital Foundation.

References

1. Cummings SR, Melton LJ. Epidemiology and outcomes of osteoporotic fractures. Lancet. 2002; 359(9319):1761–7. [PubMed: 12049882]
2. Amin S, Achenbach SJ, Atkinson EJ, Khosla S, Melton LJ 3rd. Trends in fracture incidence: a population-based study over 20 years. J Bone Miner Res. 2014; 29(3):581–9. [PubMed: 23959594]

3. Black DM, Rosen CJ. Clinical Practice. Postmenopausal Osteoporosis. N Engl J Med. 2016; 374(3): 254–62. [PubMed: 26789873]
4. Center JR, Bliuc D, Nguyen ND, Nguyen TV, Eisman JA. Osteoporosis medication and reduced mortality risk in elderly women and men. J Clin Endocrinol Metab. 2011; 96(4):1006–14. [PubMed: 21289270]
5. Clevers H, Loh KM, Nusse R. Stem cell signaling. An integral program for tissue renewal and regeneration: Wnt signaling and stem cell control. Science. 2014; 346(6205):1248012. [PubMed: 25278615]
6. Baron R, Kneissel M. WNT signaling in bone homeostasis and disease: from human mutations to treatments. Nat Med. 2013; 19(2):179–92. [PubMed: 23389618]
7. Appelman-Dijkstra NM, Papapoulos SE. Sclerostin Inhibition in the Management of Osteoporosis. Calcif Tissue Int. 2016; 98(4):370–80. [PubMed: 27016922]
8. Moester MJ, Papapoulos SE, Lowik CW, van Bezooijen RL. Sclerostin: current knowledge and future perspectives. Calcif Tissue Int. 2010; 87(2):99–107. [PubMed: 20473488]
9. Chung BD, Kayserili H, Ai M, et al. A mutation in the signal sequence of LRP5 in a family with an osteoporosis-pseudoglioma syndrome (OPPG)-like phenotype indicates a novel disease mechanism for trinucleotide repeats. Hum Mutat. 2009; 30(4):641–8. [PubMed: 19177549]
10. Salazar VS, Zarkadis N, Huang L, et al. Embryonic ablation of osteoblast Smad4 interrupts matrix synthesis in response to canonical Wnt signaling and causes an osteogenesis-imperfecta-like phenotype. J Cell Sci. 2013; 126(Pt 21):4974–84. [PubMed: 24006258]
11. McClung MR, Grauer A, Boonen S, et al. Romosozumab in postmenopausal women with low bone mineral density. N Engl J Med. 2014; 370(5):412–20. [PubMed: 24382002]
12. Yagi T, Takeichi M. Cadherin superfamily genes: functions, genomic organization, and neurologic diversity. Genes Dev. 2000; 14(10):1169–80. [PubMed: 10817752]
13. Nelson WJ, Nusse R. Convergence of Wnt, b-catenin, and cadherin pathways. Science. 2004; 303(5663):1483–7. [PubMed: 15001769]
14. Gumbiner BM. Regulation of cadherin-mediated adhesion in morphogenesis. Nat Rev Mol Cell Biol. 2005; 6(8):622–34. [PubMed: 16025097]
15. Hay E, Nouraud A, Marie PJ. N-cadherin negatively regulates osteoblast proliferation and survival by antagonizing Wnt, ERK and PI3K/Akt signalling. PLoS One. 2009; 4(12):e8284. [PubMed: 20011526]
16. Hay E, Laplantine E, Geoffroy V, et al. N-cadherin interacts with axin and LRP5 to negatively regulate Wnt/beta-catenin signaling, osteoblast function, and bone formation. Mol Cell Biol. 2009; 29(4):953–64. [PubMed: 19075000]
17. Marie PJ, Hay E, Modrowski D, Revollo L, Mbalaviele G, Civitelli R. Cadherin-mediated cell-cell adhesion and signaling in the skeleton. Calcif Tissue Int. 2014; 94(1):46–54. [PubMed: 23657489]
18. Revollo L, Kading J, Jeong SY, et al. N-cadherin restrains PTH activation of Lrp6/beta-catenin signaling and osteoanabolic action. J Bone Miner Res. 2015; 30(2):274–85. [PubMed: 25088803]
19. Castro CH, Shin CS, Stains JP, et al. Targeted expression of a dominant-negative N-cadherin in vivo delays peak bone mass and increases adipogenesis. J Cell Sci. 2004; 117(Pt 13):2853–64. [PubMed: 15169841]
20. Di Benedetto A, Watkins M, Grimston S, et al. N-cadherin and cadherin 11 modulate postnatal bone growth and osteoblast differentiation by distinct mechanisms. J Cell Sci. 2010; 123(Pt 15): 2640–8. [PubMed: 20605916]
21. Greenbaum AM, Revollo LD, Woloszynek JR, Civitelli R, Link DC. N-cadherin in osteolineage cells is not required for maintenance of hematopoietic stem cells. Blood. 2012; 120(2):295–302. [PubMed: 22323481]
22. Kostetskii I, Li J, Xiong Y, et al. Induced deletion of the N-cadherin gene in the heart leads to dissolution of the intercalated disc structure. Circ Res. 2005; 96(3):346–54. [PubMed: 15662031]
23. Dacquin R, Starbuck M, Schinke T, Karsenty G. Mouse alpha1(I)-collagen promoter is the best known promoter to drive efficient Cre recombinase expression in osteoblast. Dev Dyn. 2002; 224(2):245–51. [PubMed: 12112477]
24. Greenbaum A, Hsu YM, Day RB, et al. CXCL12 in early mesenchymal progenitors is required for haematopoietic stem-cell maintenance. Nature. 2013; 495(7440):227–30. [PubMed: 23434756]

25. Cui Y, Niziolek PJ, Macdonald BT, et al. Lrp5 functions in bone to regulate bone mass. Nat Med. 2011; 17(6):684–91. [PubMed: 21602802]
26. Chung DJ, Castro CH, Watkins M, et al. Low peak bone mass and attenuated anabolic response to parathyroid hormone in mice with an osteoblast-specific deletion of connexin43. J Cell Sci. 2006; 119(Pt 20):4187–98. [PubMed: 16984976]
27. Grimston SK, Goldberg DB, Watkins M, Brodt MD, Silva MJ, Civitelli R. Connexin43 deficiency reduces the sensitivity of cortical bone to the effects of muscle paralysis. J Bone Miner Res. 2011; 26(9):2151–60. [PubMed: 21590735]
28. Watkins MP, Norris JY, Grimston SK, et al. Bisphosphonates improve trabecular bone mass and normalize cortical thickness in ovariectomized, osteoblast connexin43 deficient mice. Bone. 2012; 51(4):787–94. [PubMed: 22750450]
29. Zhang J, Link DC. Targeting of Mesenchymal Stromal Cells by Cre-Recombinase Transgenes Commonly Used to Target Osteoblast Lineage Cells. J Bone Miner Res. 2016
30. Houlihan DD, Mabuchi Y, Morikawa S, et al. Isolation of mouse mesenchymal stem cells on the basis of expression of Sca-1 and PDGFR-alpha. Nature protocols. 2012; 7(12):2103–11. [PubMed: 23154782]
31. Parfitt AM, Drezner MK, Glorieux FH, et al. Bone histomorphometry: standardization of nomenclature, symbols, and units. Report of the ASBMR Histomorphometry Nomenclature Committee. J Bone Miner Res. 1987; 2(6):595–610. [PubMed: 3455637]
32. Watkins M, Grimston SK, Norris JY, et al. Osteoblast connexin43 modulates skeletal architecture by regulating both arms of bone remodeling. Mol Biol Cell. 2011; 22(8):1240–51. [PubMed: 21346198]
33. Di Benedetto A, Watkins M, Grimston S, et al. N-cadherin and cadherin 11 modulate postnatal bone growth and osteoblast differentiation by distinct mechanisms. Journal of cell science. 2010; 123(Pt 15):2640–8. [PubMed: 20605916]
34. Salazar VS, Zarkadis N, Huang L, et al. Embryonic ablation of osteoblast Smad4 interrupts matrix synthesis in response to canonical Wnt signaling and causes an osteogenesis-imperfecta-like phenotype. J Cell Sci. 2013; 126(Pt 21):4974–84. [PubMed: 24006258]
35. Mizoguchi T, Pinho S, Ahmed J, et al. Osterix marks distinct waves of primitive and definitive stromal progenitors during bone marrow development. Dev Cell. 2014; 29(3):340–9. [PubMed: 24823377]
36. Davey RA, Clarke MV, Sastra S, et al. Decreased body weight in young Osterix-Cre transgenic mice results in delayed cortical bone expansion and accrual. Transgenic Res. 2012; 21(4):885–93. [PubMed: 22160436]
37. Logan M, Martin JF, Nagy A, Lobe C, Olson EN, Tabin CJ. Expression of Cre Recombinase in the developing mouse limb bud driven by a Prxl enhancer. Genesis. 2002; 33(2):77–80. [PubMed: 12112875]
38. Lai CF, Cheng SL, Mbalaviele G, et al. Accentuated ovariectomy-induced bone loss and altered osteogenesis in heterozygous N-cadherin null mice. J Bone Miner Res. 2006; 21(12):1897–906. [PubMed: 17002573]
39. Marie PJ, Hay E. Cadherins and Wnt signalling: a functional link controlling bone formation. BoneKEy Rep. 2013; 2:330. [PubMed: 24422077]
40. Marie PJ, Hay E, Modrowski D, Revollo L, Mbalaviele G, Civitelli R. Cadherin-mediated cell-cell adhesion and signaling in the skeleton. Calcif Tissue Int. 2014; 94(1):46–54. [PubMed: 23657489]
41. Hay E, Dieudonne FX, Saidak Z, et al. N-cadherin/wnt interaction controls bone marrow mesenchymal cell fate and bone mass during aging. J Cell Physiol. 2014; 229(11):1765–75. [PubMed: 24664975]
42. Delise AM, Tuan RS. Analysis of N-cadherin function in limb mesenchymal chondrogenesis in vitro. Dev Dyn. 2002; 225(2):195–204. [PubMed: 12242719]
43. Tuli R, Tuli S, Nandi S, et al. Transforming growth factor-beta-mediated chondrogenesis of human mesenchymal progenitor cells involves N-cadherin and mitogen-activated protein kinase and Wnt signaling cross-talk. J Biol Chem. 2003; 278(42):41227–36. [PubMed: 12893825]

44. DeLise AM, Tuan RS. Alterations in the spatiotemporal expression pattern and function of N-cadherin inhibit cellular condensation and chondrogenesis of limb mesenchymal cells in vitro. J Cell Biochem. 2002; 87(3):342–59. [PubMed: 12397616]

45. Alfaro MP, Vincent A, Saraswati S, et al. sFRP2 suppression of bone morphogenic protein (BMP) and Wnt signaling mediates mesenchymal stem cell (MSC) self-renewal promoting engraftment and myocardial repair. J Biol Chem. 2010; 285(46):35645–53. [PubMed: 20826809]

46. Aomatsu E, Chosa N, Nishihira S, Sugiyama Y, Miura H, Ishisaki A. Cell-cell adhesion through N-cadherin enhances VCAM-1 expression via PDGFRbeta in a ligand-independent manner in mesenchymal stem cells. Int J Mol Med. 2014; 33(3):565–72. [PubMed: 24378362]

47. Genant HK, Engelke K, Bolognese MA, et al. Effects of Romosozumab Compared With Teriparatide on Bone Density and Mass at the Spine and Hip in Postmenopausal Women With Low Bone Mass. J Bone Miner Res. 2016

48. Recknor CP, Recker RR, Benson CT, et al. The Effect of Discontinuing Treatment With Blosozumab: Follow-up Results of a Phase 2 Randomized Clinical Trial in Postmenopausal Women With Low Bone Mineral Density. J Bone Miner Res. 2015; 30(9):1717–25. [PubMed: 25707611]

49. Stolina M, Dwyer D, Niu QT, et al. Temporal changes in systemic and local expression of bone turnover markers during six months of sclerostin antibody administration to ovariectomized rats. Bone. 2014; 67:305–13. [PubMed: 25093263]

50. Hay E, Buczkowski T, Marty C, Da Nascimento S, Sonnet P, Marie PJ. Peptide-based mediated disruption of N-cadherin-LRP5/6 interaction promotes Wnt signaling and bone formation. J Bone Miner Res. 2012; 27(9):1852–63. [PubMed: 22576936]

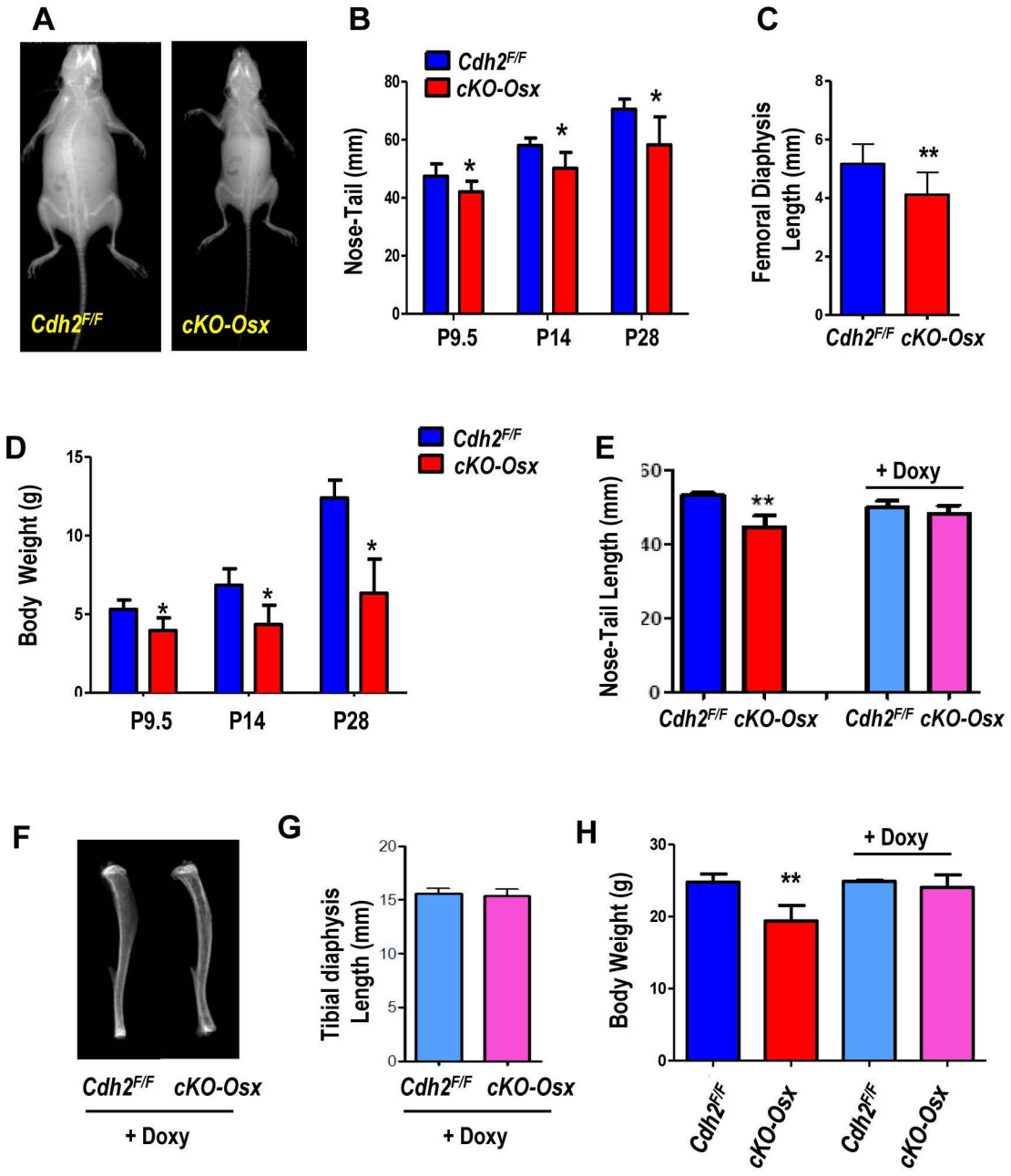

Figure 1. Skeletal growth defects in *cKO-Osx* mice are prevented by delaying *Cdh2* recombination until 1 month of age

(A) Representative radiographs of 28-day-old *Cdh2*$^{F/F}$ and *cKO-Osx* littermates. (B) Nose-to-tail length of *Cdh2*$^{F/F}$ (blue) and *cKO-Osx* (red) pups at ages P8-11 (grouped as P9.5, n=15 and 13), P13-16 (grouped as P14, n=7 and 4), or P28 (n=2 and 4). (C) Femoral diaphysis length in 10-day-old *Cdh2*$^{F/F}$ and *cKO-Osx* littermates (n=5 and 6, respectively), measured as distance between proximal and distal growth plate on plain ex-vivo X-Ray images. (D) Body weight of animals described in B. (E) Nose-to-tail length of 10-day-old *Cdh2*$^{F/F}$ and *cKO-Osx* littermates fed a regular chow (left bars) or a Doxycycline (Doxy)-containing chow (right bars) (n=6 each). (F) Representative ex-vivo radiographs of the tibia,

and (G) length of tibial diaphysis measured as distance between growth plates in Doxy-treated 2-month-old *Cdh2*$^{F/F}$ and *cKO-Osx* littermates (n=4, 3, respectively). (H) Body weight of 13–16-week-old *Cdh2*$^{F/F}$ and *cKO-Osx* male mice fed a regular chow (left bars) or Doxy-containing chow (right bars). *p<0.01 vs. *Cdh2*$^{F/F}$, two-way ANOVA for genotype and time, followed by Bonferroni post-hoc test; **p<0.05 vs. *Cdh2*$^{F/F}$, ANOVA.

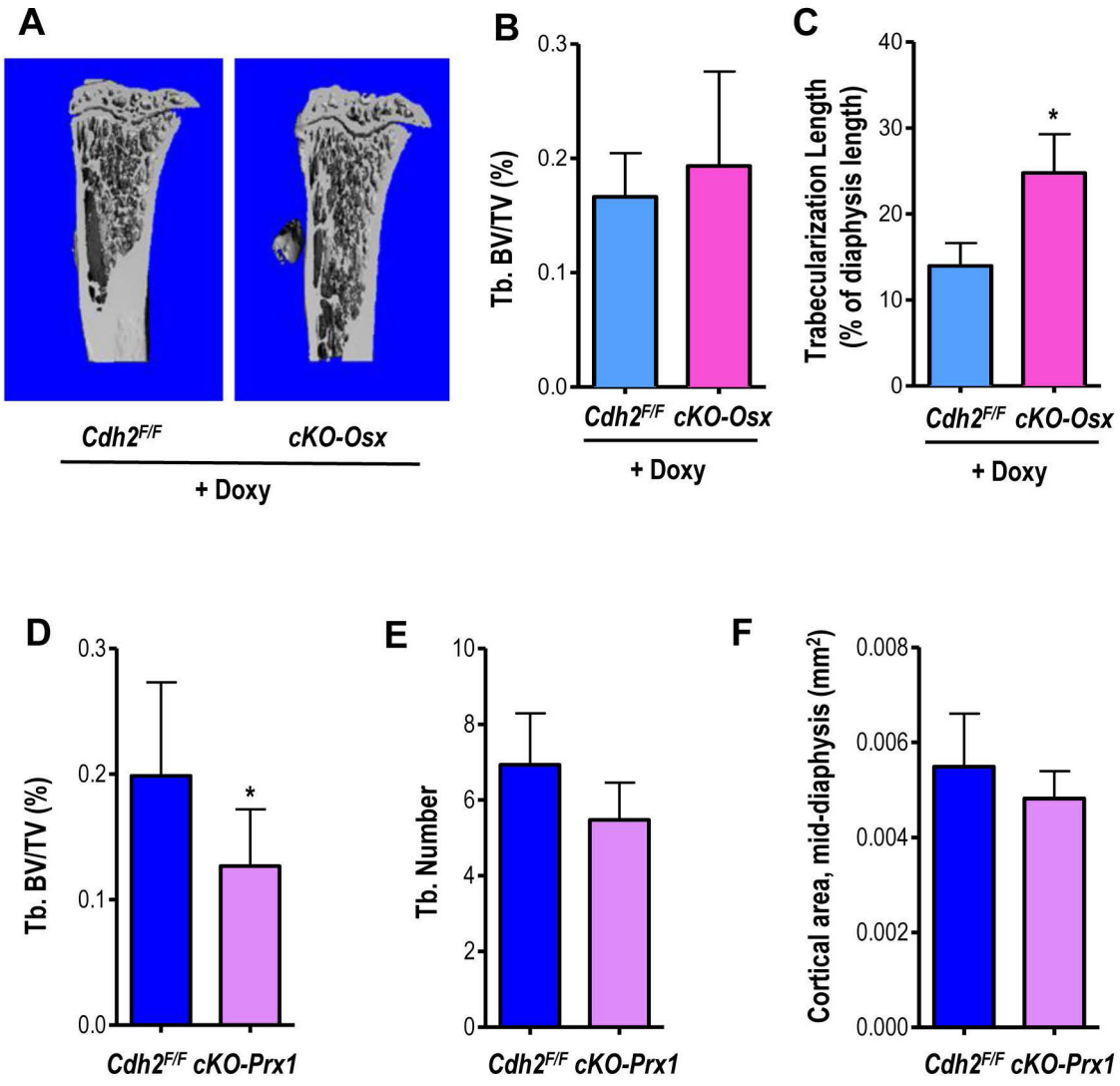

Figure 2. Delayed *Cdh2* ablation prevents the low bone mass phenotype present in mice with embryonic *Cdh2* ablation

(A) Representative μCT images of tibiae of 2-months-old, Doxycycline (Doxy)-fed, male *Cdh2*$^{F/F}$ and *cKO-Osx* mice. (B) Volumetric trabecular bone volume/total bone volume (BV/TV) and (C) trabecularization of the diaphysis, as percent of diaphyseal length in the two groups of animals. (D) Volumetric BV/TV, (E) trabecular number (Tb. N), and (F) cortical area at the mid-diaphysis measured by in vivo μCT in 2-month-old male *Cdh2*$^{F/F}$ and *Cdh2*^{Prx} littermates (n=7, 8, respectively). Similar results (not shown) were observed in females *p<0.05 vs. *Cdh2*$^{F/F}$, Student's t-test.

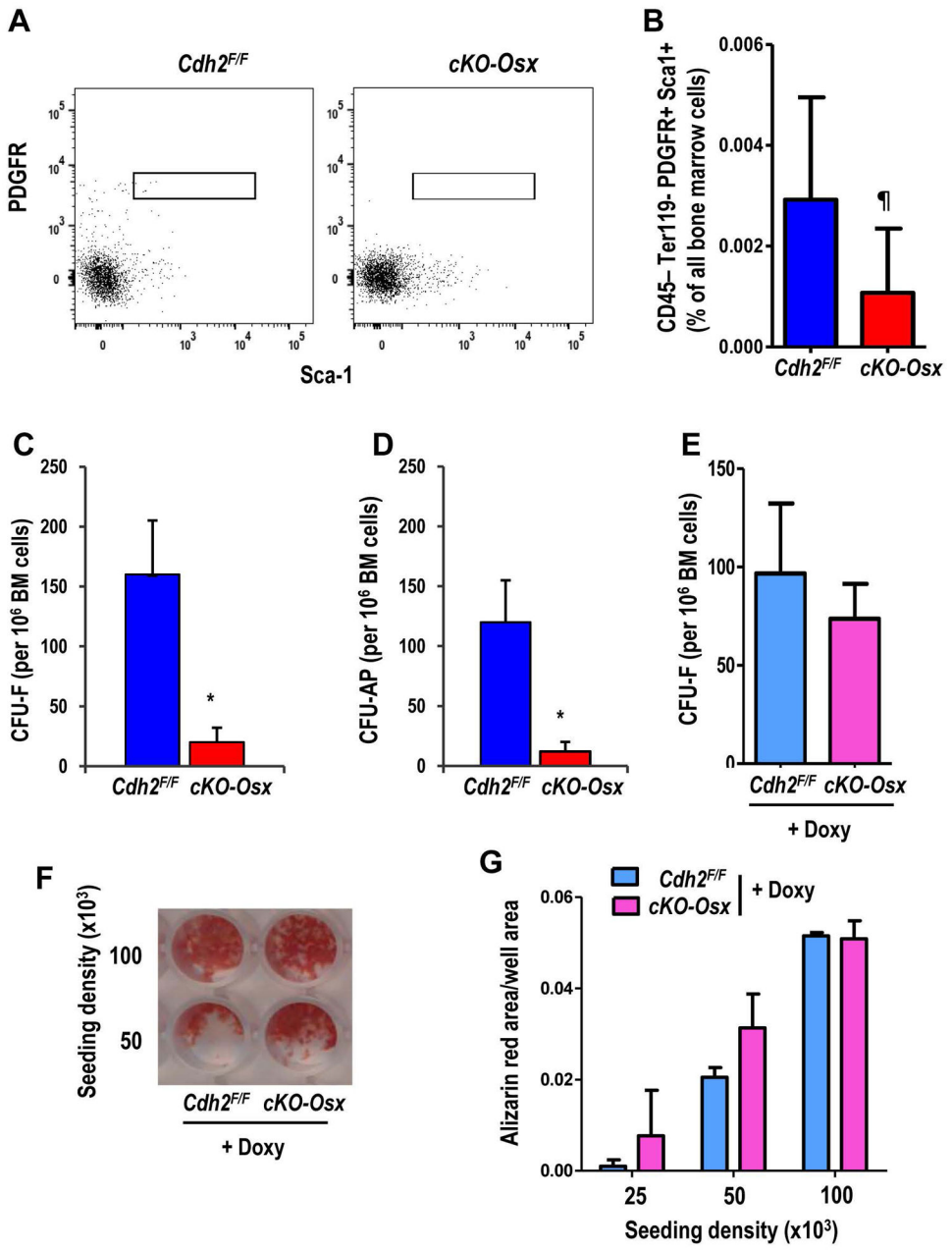

Figure 3. Loss of N-cadherin reduces the number of bone marrow cells with MSPC features

(A) Representative flow cytometry plots of bone marrow stromal cells from *Cdh2*$^{F/F}$ (left) and *cKO-Osx* (right) mice analyzed for Sca-1 (x-axis) and PDGFRβ (y-axis) in the CD45− Ter119− CD31− population. (B) Percent of CD45− Ter119− CD31− PDGFRβ + Sca-1+ (PβS) cells in the bone marrow of 3-week-old *Cdh2*$^{F/F}$ (blue, n=4) and *cKO-Osx* (red, n=8) littermates [$p<0.05$; Wilcoxon ranking test, to include samples with 0 gated events]. (C) Colony forming units-fibroblast (CFU-F), and (D) CFU-alkaline phosphatase (CFU-AP) in bone marrow cells from mice of the two genotypes, as indicated (*$p<0.05$; Student's t test). (E) CFU-F cells in bone marrow cells from Doxycycline (Doxy)-fed (until P28) *Cdh2*$^{F/F}$ (n=3) and *cKO-Osx* (n=4) mice ($p>0.10$; Student's t test). (F) Representative example of

alizarin red staining of bone marrow cell cultures from Doxy-treated *Cdh2*$^{F/F}$ and *cKO-Osx* mice after 3 weeks in osteogenic media, at 2 seeding densities. (G) Quantification of alizarin red staining as exemplified in D, in bone marrow cell cultured from Doxy-treated *Cdh2*$^{F/F}$ (n=2) and *cKO-Osx* mice (n=6), seeded at 3 different densities (each condition run in duplicate; $p>0.10$, two-way ANOVA for genotype and seeding density).

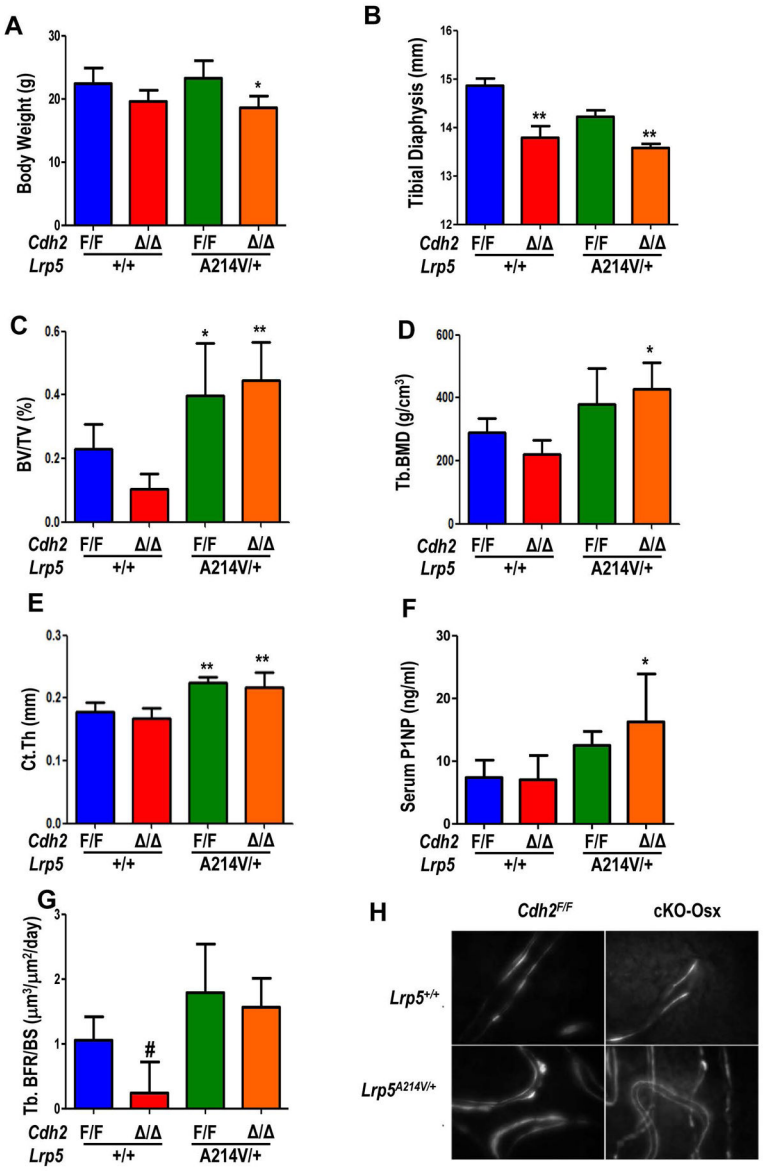

Figure 4. The gain-of-function *Lrp5*^{A214V} mutant fully rescues the low bone mass but not the growth defect of *cKO-Osx* mice

(A) Body weight of 2-month-old male *Cdh2*$^{F/F}$ and *cKO-Osx* (Δ/Δ) in a wild type *Lrp5* background (blue, red, respectively), compound mutant *Cdh2*$^{F/F}$;*Lrp5*$^{A214V/+}$ (green), and *cKO-Osx;Lrp5*$^{A214V/+}$ (orange) mice (n=6/genotype). (B) Tibial diaphysis length in 3-month-old mice of the same genotypes (n=5–6/genotype). (C) Volumetric bone volume/tissue volume (BV/TV), (D) trabecular bone mineral density (Tb.BMD), and (E) cortical thickness (Ct.Th) of the femur by µCT analysis of 3-month-old mice (n=6/genotype). (F) Serum levels of type I pro-collagen N-terminal propeptide (P1NP) at 2 months of age (n=3–6/group). (G) Trabecular bone volume/bone surface (BFR/BS, n=2–4/group), and (H) representative fluorescence micrographs of Doxycycline-labeled undecalcified sections of distal femurs, showing occasional double-labels in *Cdh2*$^{F/F}$ bones, only single labels in *cKO-Osx*, but abundant double-labels in *Lrp5*$^{A214V/+}$ and compound *cKO-Osx;Lrp5*$^{A214V/+}$

mutants. One-way ANOVA, *p<0.05 **p<0.01 vs. $Cdh2^{F/F}$ by Dunnett's post-hoc test, #p<0.05 vs. $Cdh2^{F/F}$;$Lrp5^{A214V/+}$ by Bonferroni test. Results shown are for male animals; similar results were obtained in females.

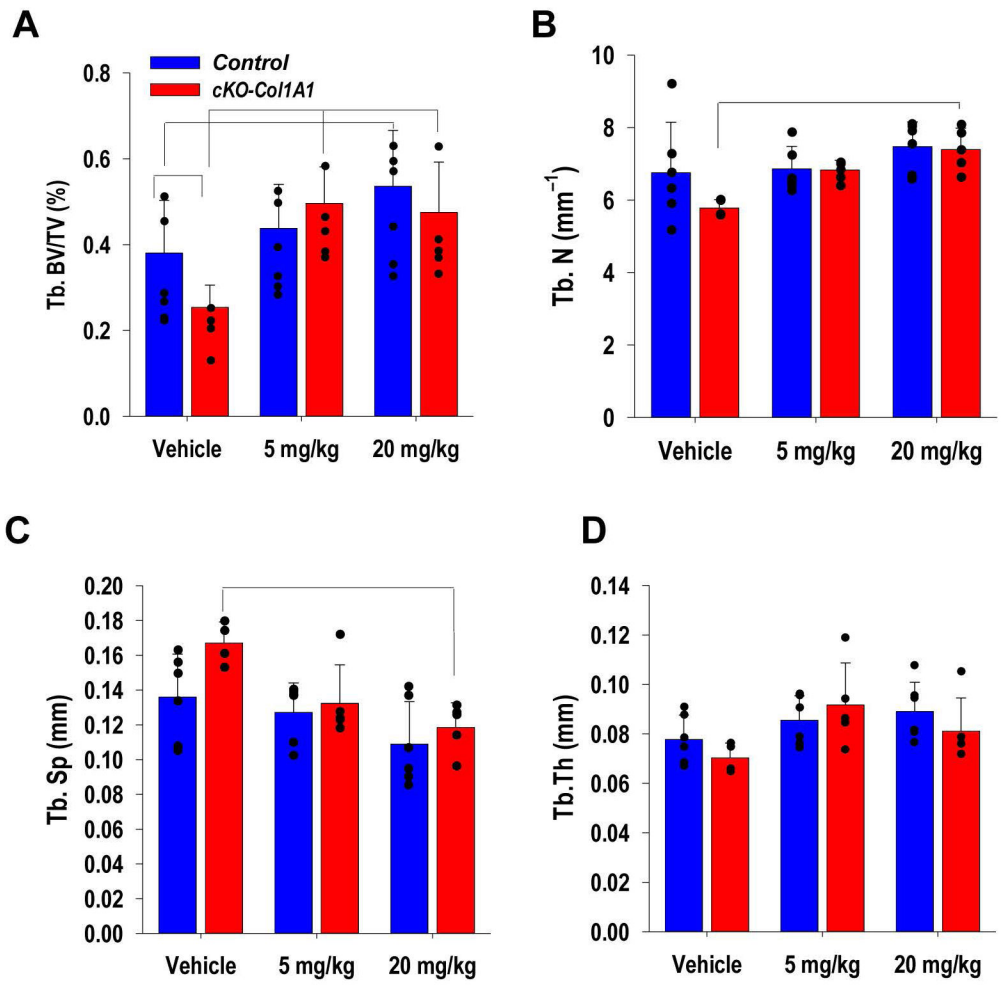

Figure 5. *Cdh2* ablation in osteoblasts enhances trabecular bone accrual in response to anti-Dkk1 antibody administration

(A) Volumetric trabecular bone volume/tissue volume (BV/TV), (B) trabecular number, (C) trabecular spacing, and (D) trabecular thickness by μCT in tibiae of control (blue; n=11 *Cdh2* $^{+/+}$;*Col1A1-Cre*$^{+}$ and 6 *Cdh2*$^{+/+}$) and *cKO-Col1A1* (red; n=15) 2-month-old male mice treated with vehicle or αDkk1 antibody 5 or 20 mg/kg body weight, 3 times/week for 4 weeks (n=5–7/group). Similar results were observed in female mice (not shown). Brackets indicate $p<0.05$ between groups (ANOVA, followed by Bonferroni post-hoc test for each genotype group).